



## **Practical aspects of sensitivity function approximation for dynamic models**

DIRK J.W. DE PAUW\* and PETER A. VANROLLEGHEM

Biomath, Department of Applied Mathematics, Biometrics and Process Control,  
Ghent University, Coupure Links 653, 9000 Ghent, Belgium

Sensitivity analysis can be used to quantify the magnitude of the dependency of model predictions on certain modelling assumptions, e.g. parameter values, initial conditions or inputs. The finite difference method, a local sensitivity analysis technique, is discussed in detail and situated among other methods. A lot of attention is paid to the practical issues concerning the implementation of this technique, more specifically the effect of nonlinearities of the model and numerical problems. The influence of the perturbation factor on the sensitivity calculations is investigated and different criteria are proposed to assess the quality of the sensitivity functions. A threshold value with good probability of detecting faulty sensitivity function calculations was found for one of these criteria, implying that the method can be automated.

*Keywords:* Sensitivity analysis; Finite difference; Dynamic models

### **1. Introduction**

Sensitivity analysis studies the ‘sensitivity’ of the outputs of a system to changes in the parameters, inputs or initial conditions which are often poorly known. Sensitivity analysis can be divided into two large categories: local and global sensitivity analysis. Local sensitivity analysis methods refer to small changes of parameters, while global methods refer to the effect of simultaneous, possibly orders-of-magnitude parameter changes. Both categories will be described in section 2 of this paper, with the focus on local sensitivity analysis techniques. One of these sensitivity analysis techniques, the finite difference method, will be discussed in section 4 and illustrated for models described in section 3. The finite difference technique is often used to obtain a sensitivity measure, most of the time without considering the nonlinearity of the model or the round-off error introduced by the output calculations. These influences will be analysed and discussed in detail.

---

\*Corresponding author. Email: [dirk.depauw@biomath.ugent.be](mailto:dirk.depauw@biomath.ugent.be)

## 2. Sensitivity analysis

The general form of the systems that will be discussed is given by following equation:

$$\frac{dy}{dt} = f(y, \theta), \quad (1)$$

where  $y$  is an  $n$ -dimensional vector of state variables,  $\theta$  is the  $p$ -dimensional vector of system parameters (which can include the initial conditions  $y^0$  and input variables) and  $t$  is the independent variable.

The sensitivity of a state variable  $y$  to a parameter  $\theta$  can be expressed as a sensitivity function (equation (2)). A state variable  $y$  is called sensitive to  $\theta$  if small changes in  $\theta$  produce significant changes in  $y$ . On the other hand, a variable  $y$  is called insensitive to  $\theta$  if changes in  $\theta$  produce insignificant changes in  $y$ .

$$S(t) = \frac{\partial y(t)}{\partial \theta}. \quad (2)$$

This partial derivative can be analytically solved if the analytical solution of equation (1) is known. Unfortunately, this is rarely the case and numerical methods have to be used in order to approximate the sensitivity function (equation (2)). Since sensitivity functions are used in several applications like optimal experimental design, model reduction, etc., it is of great importance that a correct approximation of the sensitivity function is calculated in order for the applications, in which the sensitivity functions are used, to produce accurate results. Local sensitivity analysis techniques evaluate this partial derivative at one specific set of parameter values, also called the nominal parameter set. On the other hand global techniques evaluate this partial derivative in various points of the parametric domain. Both local and global analysis are useful in studying the behaviour of a system since each has advantages and disadvantages. For detailed reviews of existing sensitivity techniques reference is made to Turanyi [1] and Rabitz *et al.* [2]. The main focus of this paper will be the local sensitivity analysis techniques.

Various techniques for local sensitivity analysis will be described here, which are (a) the finite difference method, (b) the direct differential method, (c) the Green's function method, (d) the polynomial approximation method and (e) automatic differentiation.

The simplest way of calculating local sensitivities is to use the finite difference approximation. This technique is also called the brute force method or indirect method. It is very easy to implement because it requires no extra code beyond the original model solver. The partial derivative defined in equation (2) can be mathematically formulated by the equation given below (forward difference):

$$\frac{\partial y_i}{\partial \theta_j} = \lim_{\Delta \theta_j \rightarrow 0} \frac{y_i(t, \theta_j + \Delta \theta_j) - y_i(t, \theta_j)}{\Delta \theta_j}. \quad (3)$$

This equation is only valid if an infinitesimal variation (perturbation) of the parameters is considered, inputs or initial conditions ( $\Delta \theta_j \rightarrow 0$ ). Equation (3) shows that the application of the finite difference method requires the solution of the model (equation (1)) using the nominal value of the parameters  $y_i(t, \theta_j)$  and  $p$  solutions of the equations using perturbed parameters  $y_i(t, \theta_j + \Delta \theta_j)$ . It should be noted that only one parameter is perturbed at a time while all others are kept at their nominal value. The sensitivities obtained actually belong to the  $(\theta + \Delta \theta/2)$  parameter set because equation (3) can also be seen as the average of the sensitivities of the model output  $y_i$  at  $\theta_j$  and  $\theta_j + \Delta \theta_j$ . If the sensitivity coefficients associated with the nominal values  $\theta_j$

are required, equation (3) should be modified into the central difference formula (equation (4)) which requires  $2p$  solutions.

$$\frac{\partial y_i}{\partial \theta_j} \approx \frac{y_i(t, \theta_j + \Delta\theta_j) - y_i(t, \theta_j - \Delta\theta_j)}{2\Delta\theta_j}. \quad (4)$$

The finite difference technique was found to be too calculation intensive, especially in cases where sensitivities to many parameters were required. Therefore Atherton *et al.* [3] developed the direct method for sensitivity analysis. Differentiation of equation (1) with respect to  $\theta_j$  yields the following set of sensitivity differential equations. The solution of these equations results in the sensitivity functions:

$$\frac{d}{dt} \frac{\partial y}{\partial \theta_j} = \frac{\partial f}{\partial y} \frac{\partial y}{\partial \theta_j} + \frac{\partial f}{\partial \theta_j}. \quad (5)$$

The term  $\partial f / \partial y$  of equation (5) is recognized as the Jacobian  $J$  of the original system given by equation (1). Equations (1) and (5) are coupled through  $\partial f / \partial y$  and  $\partial f / \partial \theta$ . This means that the solution of equation (5) requires the knowledge of the solution of equation (1) in all points where the ODE (ordinary differential equation) solver calculates the right-hand side of equation (5). A link between these two sets of equations can be made in one of the following ways.

- (i) Solve equations (1) and (5) for every parameter  $\theta$  simultaneously, which requires the solution of  $(p+1)n$  ODEs. The direct solution of this large system is inefficient. Although a solver has been built for these systems, based on the decomposed direct method [4], it is not used very often.
- (ii) Solve the couple of equations (1) and (5), which requires the solution of  $2n$  ODEs  $p$  times (for every parameter) [5]. This version is the simplest to code, but is the least economical and might cause numerical problems due to ill-conditioned Jacobian matrices [6–8].
- (iii) The solution of equations (1) and (5) can be decoupled. First, differential equations (1) are solved and the results are stored in a table. Then equations (5) are solved using the values stored in the table. If values are required at times without tabulated values, they are computed by interpolation [3,6,8,9]. An improved version of this decoupled method was introduced by Dunker [10,11]. His method made use of the fact that the Jacobian matrix of equations (1) and (5) is the same and that it only has to be triangulated once every time step.

The difficulties of solving the large sets of differential equations led to the development of the Green's function method, also called the variational method [12]. This method makes use of the fact that the sensitivities (equation (5)) can be expressed in integral, rather than differential form.

$$\frac{\partial y(t)}{\partial \theta} = K(t, 0) \frac{\partial y(0)}{\partial \theta} + \int_0^t K(t, \tau) \frac{\partial f(\tau)}{\partial \theta} d\tau. \quad (6)$$

In this equation,  $K(t, \tau)$  is an  $n \times n$  Green's function matrix or kernel, given by

$$\frac{d}{dt} K(t, \tau) - J(t) K(t, \tau) = 0, \quad t > \tau, \quad (7a)$$

$$K(\tau, \tau) = I. \quad (7b)$$

There are a number of variations of the Green's function method and they differ among each other in the calculation of the matrix  $K$ . Probably the most used method is

the GFM/AIM method (Analytically Integrated Magnus). This method approximates  $K$  by a matrix exponential [8]. It is beyond the scope of this paper to go into more detail on these solving techniques. In all Green's function methods, the numerical effort is proportional to the number of variables and not the number of parameters. So this method should be preferred when the number of parameters is large compared to the number of variables. When the number of variables is much larger than the number of parameters, direct differential methods should be used.

In 1983, another local sensitivity analysis technique was developed by Hwang [13,14] called the polynomial approximation method. The basic idea behind this method is that the temporal behaviour of the solution of equation (1) is approximated by Lagrange interpolation polynomials. From these polynomials the sensitivity coefficients can easily be calculated. However, to our knowledge, this method was never applied to a real problem.

Recently, a technique called automatic differentiation has gained a lot of attention. Automatic differentiation techniques are based on the fact that every function, no matter how complicated, is executed on a computer as a sequence of elementary functions. By applying the chain rule of differentiation repeatedly to the composition of these elementary operations, one can compute the derivative information exactly and in a completely automated fashion. This method produces compilable code that evaluates derivatives up to machine precision with a minimum of human effort [15].

All the above techniques except for the finite difference technique have one thing in common. They all require complex manipulations of the model equations. In many studies this is not practically feasible because the models are too complicated or the model equations are not directly accessible (e.g. because they are compiled in executable commercial code). This is the basic reason why the finite difference method, although inefficient, is still used very often. The practical issues concerning this sensitivity analysis technique will be discussed in section 4.

### 3. Models under study

In order to illustrate some practical issues concerning the finite difference method, four different models will be used ranging from a very simple model to more complicated models. All models were implemented in the modelling and simulation tool WEST [16] which was also used to perform the sensitivity analysis.

#### 3.1 Monod model

Monod kinetics were used in a simple model (equations (8) and (9)).

$$\frac{dS}{dt} = -\frac{1}{Y} \frac{\mu_{\max} S}{K_S + S} X, \quad (8)$$

$$\frac{dX}{dt} = \frac{\mu_{\max} S}{K_S + S} X - K_d X. \quad (9)$$

$S$  and  $X$  represent the substrate and the biomass concentration respectively, both expressed as  $\text{mgCOD l}^{-1}$ .  $\mu_{\max}$  ( $\text{h}^{-1}$ ) is the maximum specific growth rate,  $Y$  (—) is the yield coefficient,  $K_d$  ( $\text{h}^{-1}$ ) is a decay coefficient and  $K_S$  ( $\text{mgCOD l}^{-1}$ ) is the half saturation concentration of the substrate at which the biomass grows at half the growth

rate. The nominal parameter values and initial conditions are listed in table 1. Figures 1 and 2 show simulation results of the substrate  $S$  and biomass  $X$  concentration. For this model the sensitivity of both variables ( $S$  and  $X$ ) to the four parameters is investigated (8 sensitivity functions).

### 3.2 Anaerobic digestion model

A more complex anaerobic digestion model was also considered [17]. This model is a two-step (acidogenesis–methanization) mass-balance model describing the growth of two biomass species: acidogenic bacteria ( $X_1$ ,  $\text{g l}^{-1}$ ) and methanogenic bacteria ( $X_2$ ,  $\text{g l}^{-1}$ ). In a first step, the acidogenic bacteria consume organic substrate ( $S_1$ ,  $\text{g l}^{-1}$ ) and produce  $\text{CO}_2$  ( $\text{m}^3 \text{d}^{-1}$ ) and volatile fatty acids ( $S_2$ ,  $\text{mmol l}^{-1}$ ). The methanogenic bacteria use the volatile fatty acids in a second step for growth and produce  $\text{CO}_2$  and methane ( $\text{CH}_4$ ,  $\text{m}^3 \text{d}^{-1}$ ). Alkalinity and  $pH$  (–) are also modelled because of their importance in anaerobic digestion processes. Overall this model consists of 6 differential equations and 19 parameters. Figures 3 and 4 show the dynamics of the model for the volatile fatty acid concentration  $S_2$  and the total gas production  $Q_T$  ( $\text{m}^3 \text{d}^{-1}$ ) (sum of  $\text{CO}_2$  and  $\text{CH}_4$  production rates).

For the sensitivity analysis study, 3 variables were selected: the volatile fatty acids concentration  $S_2$ , the total gas production  $Q_T$  and the  $pH$ . The sensitivity of these variables to 6 parameters was investigated: three kinetic parameters related to the volatile fatty acids ( $k_1$  (–),  $k_2$  ( $\text{mmol g}^{-1}$ ) and  $k_3$  ( $\text{mmol g}^{-1}$ )), the growth rate of the methanogenic bacteria ( $\mu_{2\text{max}}$ ,  $\text{d}^{-1}$ ), the half saturation constant of the volatile fatty acids ( $K_{S_2}$ ,  $\text{mmol l}^{-1}$ ) and the fraction of biomass in the liquid phase ( $\alpha$ , –). Combining the 3 variables and the 6 parameters resulted in 18 sensitivity functions.

### 3.3 SBR model

The third model used was a sequencing batch reactor (SBR) model describing nitrogen and phosphorous removal [18]. This activated sludge model was built on the basis of Activated Sludge Model No. 1 and 2d [19,20]. Nitrogen transformations were incorporated as an integral module following an approach similar to ASM1. The particulate nitrogen is first hydrolysed to soluble organic nitrogen and then ammonified to ammonia by heterotrophic biomass. The model consists of 89 parameters and 22 differential equations. The oxygen and phosphate dynamics in the SBR for a complete cycle with anaerobic/aerobic/anoxic/aerobic phases are illustrated in figures 5 and 6.

Table 1. Nominal parameters and initial conditions for the Monod model.

| Name               | Unit                  | Value |
|--------------------|-----------------------|-------|
| $\mu_{\text{max}}$ | $\text{h}^{-1}$       | 0.5   |
| $K_S$              | $\text{mgCOD l}^{-1}$ | 20    |
| $Y$                | –                     | 0.5   |
| $K_d$              | $\text{h}^{-1}$       | 0.03  |
| $S_0$              | $\text{mgCOD l}^{-1}$ | 10    |
| $X_0$              | $\text{mgCOD l}^{-1}$ | 0.1   |

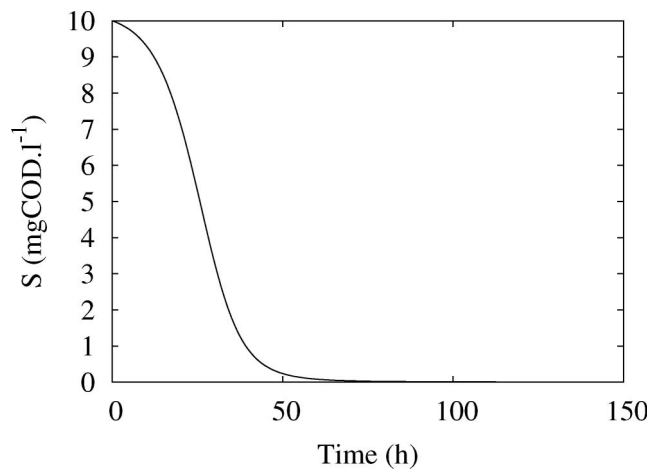


Figure 1. Simulated substrate concentration for the Monod model using the nominal parameters.

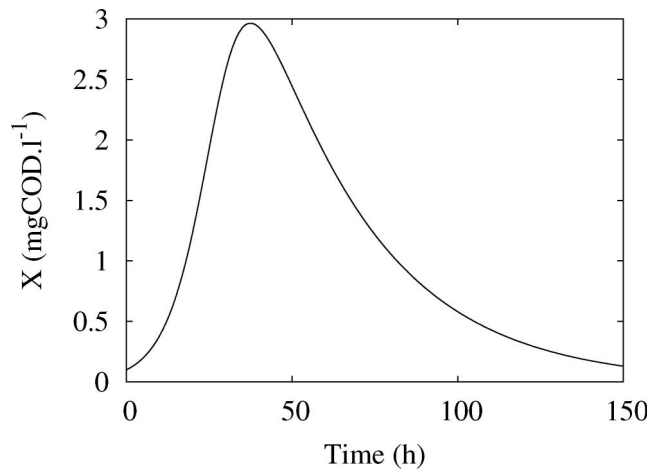


Figure 2. Simulated biomass concentration for the Monod model using the nominal parameters.

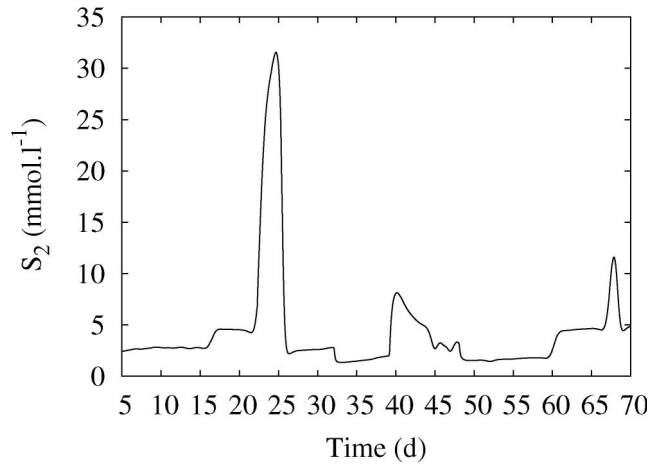


Figure 3. Simulated volatile fatty acid concentration  $S_2$  for the anaerobic digestion model.

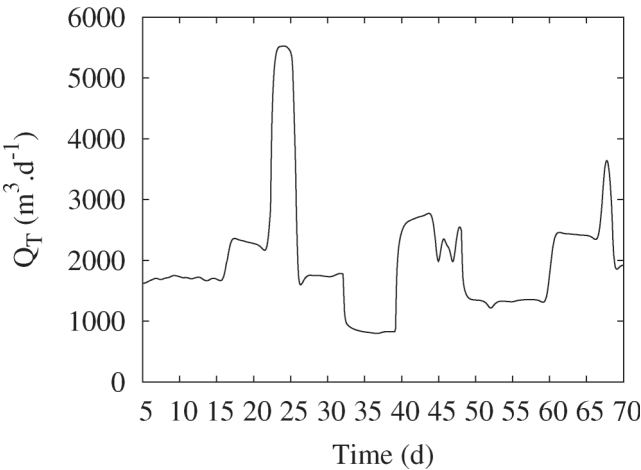


Figure 4. Simulated total gas production  $Q_T$  for the anaerobic digestion model.

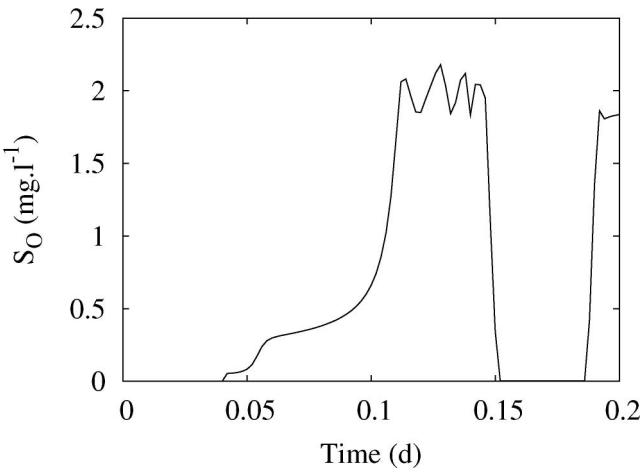


Figure 5. Simulated oxygen concentration in the SBR reactor.

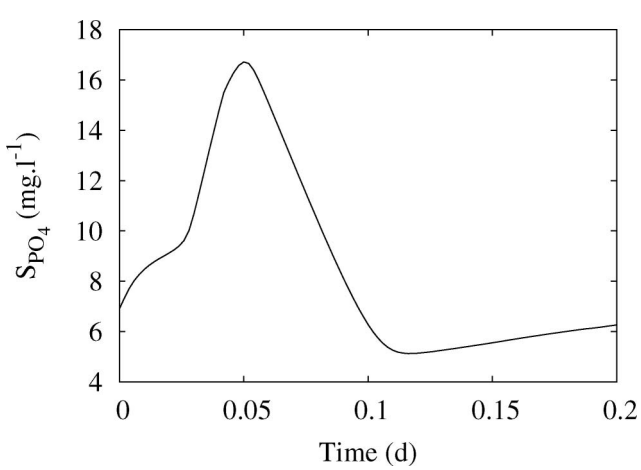


Figure 6. Simulated phosphate concentration in the SBR reactor.

From this model 4 variables and 6 parameters were selected to form 24 sensitivity functions. The selected variables were important nutrients measured in the reactor: ammonia ( $S_{\text{NH}}$ ,  $\text{mg l}^{-1}$ ), nitrate ( $S_{\text{NO}_3}$ ,  $\text{mg l}^{-1}$ ), phosphate ( $S_{\text{PO}_4}$ ,  $\text{mg l}^{-1}$ ) and oxygen ( $S_{\text{O}}$ ,  $\text{mg l}^{-1}$ ). The parameters were: the yield for heterotrophic biomass ( $Y_{\text{H}}$ ,  $-$ ), the hydrolysis rate constant ( $k_{\text{h}}$ ,  $\text{d}^{-1}$ ), the anoxic yield coefficient for heterotrophs ( $Y_{\text{HNO}_3}$ ,  $-$ ), the autotrophic yield coefficient ( $Y_{\text{NH}}$ ,  $-$ ), the rate constant of polyphosphate storage ( $Q_{\text{PP}}$ ,  $\text{d}^{-1}$ ) and the yield coefficient for phosphate release ( $Y_{\text{PO}_4}$ ,  $-$ ).

### 3.4 Benchmark model

Finally, the complex COST Simulation Benchmark model [21] was used. It is a wastewater treatment model that was designed to provide an unbiased basis for comparison of control strategies without reference to a particular wastewater treatment facility. It was also successfully used for comparing different simulation packages in the wastewater community.

The Simulation Benchmark has five biological tanks in series and a secondary settling tank. The biological tanks are modelled by the Activated Sludge Model No. 1 (ASM1) [19]. ASM1 has 13 components and 8 processes describing growth and decay of biomass, hydrolysis of organic compounds and ammonification. The secondary settler is modelled using the 1D settling model of Takacs *et al.* [22]. The model consists of 145 ( $5 \times 13 + 80$ ) differential equations. The plant layout is shown in figure 7. Figures 8 and 9 show the typical dynamics of the treatment plant for the effluent concentrations of nitrate and readily biodegradable substrate.

From this model, 5 variables and 8 parameters were selected for the sensitivity analysis study. Three effluent variables were selected: ammonia ( $S_{\text{NH}}$ ,  $\text{mg l}^{-1}$ ), nitrate ( $S_{\text{NO}_3}$ ,  $\text{mg l}^{-1}$ ) and readily biodegradable substrate ( $S_{\text{S}}$ ,  $\text{mg l}^{-1}$ ). In reactor 3 of the system, two biomass components were also selected: active heterotrophic biomass ( $X_{\text{B,H}}$ ,  $\text{mg l}^{-1}$ ) and active autotrophic biomass ( $X_{\text{B,A}}$ ,  $\text{mg l}^{-1}$ ). Four biological parameters were selected: the maximum heterotrophic growth rate ( $\mu_{\text{mH}}$ ,  $\text{d}^{-1}$ ), maximum autotrophic growth rate ( $\mu_{\text{mA}}$ ,  $\text{d}^{-1}$ ), heterotrophic yield ( $Y_{\text{H}}$ ,  $-$ ) and autotrophic yield ( $Y_{\text{A}}$ ,  $-$ ). Besides these, four physical parameters of the clarifier model were also evaluated: the clarifier surface ( $A$ ,  $\text{m}^2$ ), the clarifier height ( $H$ ,  $\text{m}$ ), the maximum settling velocity ( $v_0$ ,  $\text{m d}^{-1}$ ) and the non-settleable fraction ( $f_{\text{ns}}$ ,  $-$ ). The sensitivity functions of each of these variables to each of these parameter were calculated (for days 117–120), resulting in a total of 40 sensitivity functions.

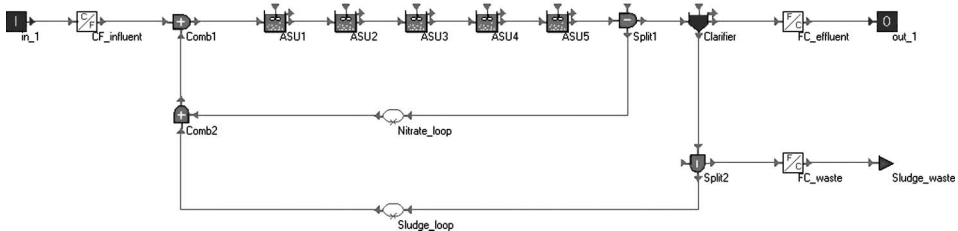


Figure 7. The plant layout of the Benchmark model.



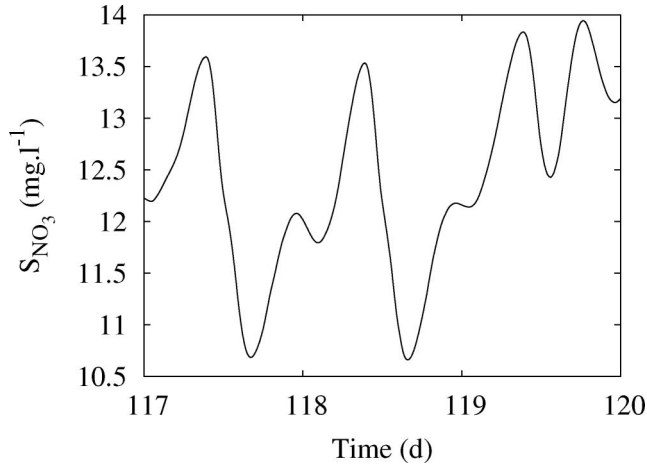


Figure 8. Simulated effluent nitrate concentration of the Benchmark treatment plant.

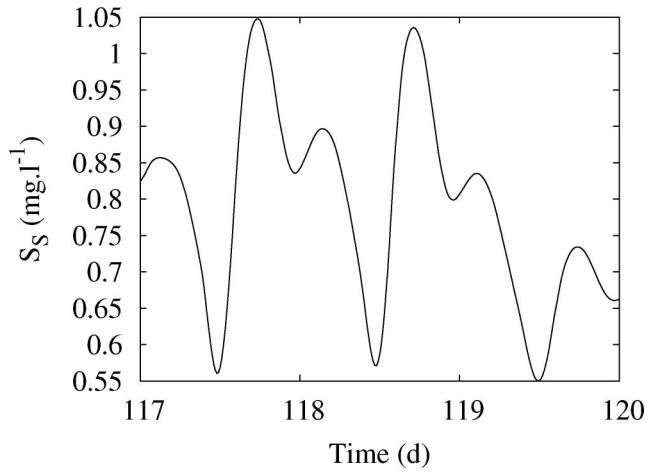


Figure 9. Simulated effluent readily biodegradable substrate concentration of the Benchmark treatment plant.

#### 4. Practical aspects of the finite difference method

##### 4.1 Theoretical background

Equation (3), which forms the basis of the finite difference method, was implemented as follows:

$$\frac{\partial y}{\partial \theta_j} \approx \frac{y(t, \theta_j + \Delta \theta_j) - y(t, \theta_j)}{\Delta \theta_j}, \quad (10)$$

where  $\Delta \theta_j$  is the change of the parameter value. Practically  $\Delta \theta_j$  was implemented as the nominal parameter value  $\theta_j$  multiplied by a user-defined perturbation factor  $\xi$ . As will be shown below, the choice of this perturbation factor will determine the quality of the sensitivity function. Equation (10) is only equivalent to equation (3) if the perturbation

factor approaches 0. From a theoretical point of view this is correct but numerically this can never be achieved because of the limited precision of the calculations. If the perturbation factor is taken too small it will result in numerical inaccuracies. On the other hand,  $\xi\theta_j$  should not become too large because then the nonlinearity of the model will start to play an important role in the sensitivity calculations. Example sensitivity functions for each model are shown in figures 10 to 13.

The practical implementation of equation (10) has two major drawbacks. The resulting sensitivity function relates to the  $(\theta_j + \xi\theta_j/2)$  parameter set and it does not provide any information on the quality of the sensitivity function. As already mentioned in section 2, if sensitivities are required around the nominal values of the parameters then the central difference formula should be used (equation (4)). Although this method requires  $2p$  model evaluations, it also provides additional information concerning the quality of the sensitivity function. Rather than just making two

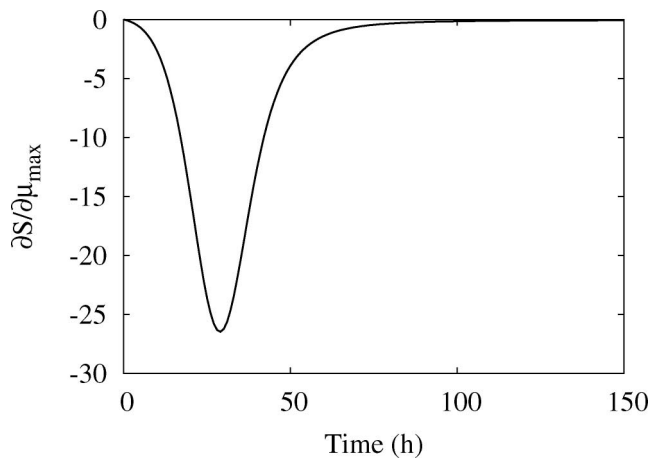


Figure 10. Sensitivity of the substrate concentration ( $S$ ) of the Monod model to the maximum growth rate ( $\mu_{\max}$ ) calculated for a perturbation factor of  $1E-07$ .

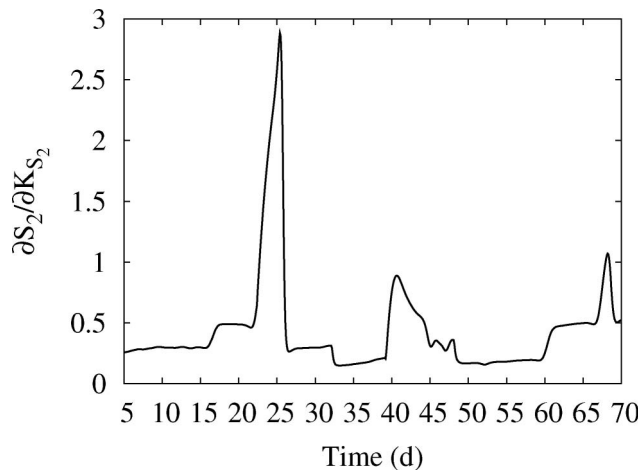


Figure 11. Sensitivity of the volatile fatty acid concentration ( $S_2$ ) of the anaerobic digestion model to the half saturation constant of the volatile fatty acids ( $K_{S_2}$ ) calculated for a perturbation factor of  $1E-03$ .

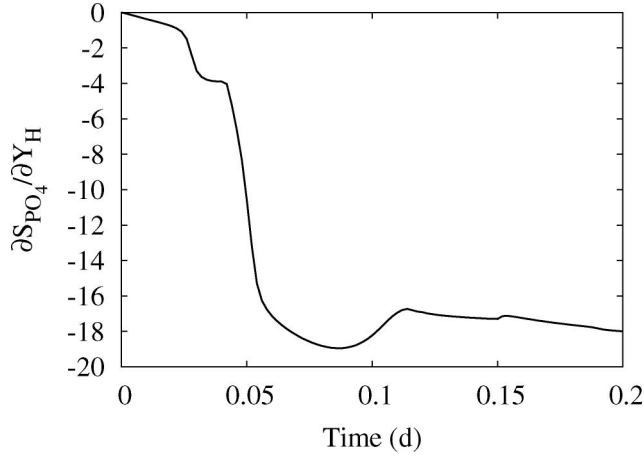


Figure 12. Sensitivity of the phosphate concentration ( $S_{PO_4}$ ) of the SBR model to the heterotrophic yield ( $Y_H$ ) calculated for a perturbation factor of  $1E-04$ .

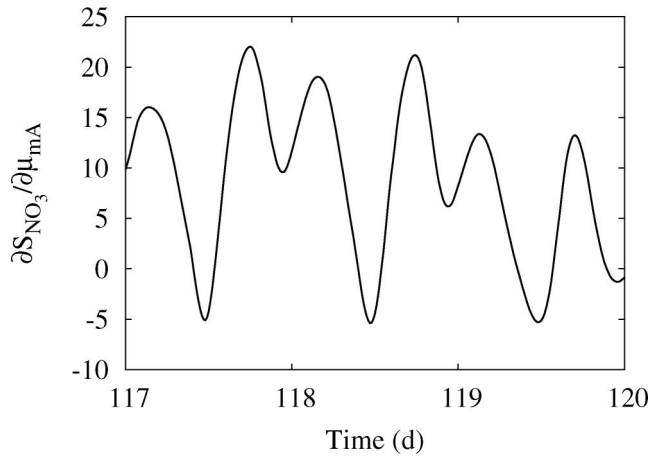


Figure 13. Sensitivity of the nitrate concentration ( $S_{NO_3}$ ) of the Benchmark model to the maximum autotrophic growth rate ( $\mu_{MA}$ ) calculated for a perturbation factor of  $1E-03$ .

evaluations of  $y(t, \theta)$  and applying equation (4), the central difference is obtained by calculating (and averaging) two sensitivity functions. The first sensitivity function is calculated by increasing the nominal parameter value by  $\xi\theta_j$ , the second sensitivity function is calculated by decreasing the nominal parameter value by  $\xi\theta_j$ .

$$\frac{\partial y}{\partial \theta_{j+}} = \frac{y(t, \theta_j + \xi\theta_j) - y(t, \theta_j)}{\xi\theta_j}, \quad (11a)$$

$$\frac{\partial y}{\partial \theta_{j-}} = \frac{y(t, \theta_j) - y(t, \theta_j - \xi\theta_j)}{\xi\theta_j}. \quad (11b)$$

To calculate the centralized sensitivity function the average of both sensitivity functions is taken.

## 4.2 Quantifying the sensitivity calculations quality

To make the numerical error and the error introduced by the nonlinearity of the model as small as possible the difference between the two sensitivity functions (equations (11a) and (11b)) should be minimal and this can be used to select the proper perturbation factor. Several criteria can be used to quantify this difference.

- (i) Sum of squared errors (SSE).

$$\frac{\sum \left( \frac{\partial y}{\partial \theta_+} - \frac{\partial y}{\partial \theta_-} \right)^2}{N}. \quad (12)$$

For this criterion, the squared error between both sensitivity functions is calculated and summed over all times where the sensitivity is desired ( $N$ ).

- (ii) Sum of absolute errors (SAE).

$$\frac{\sum \left| \frac{\partial y}{\partial \theta_+} - \frac{\partial y}{\partial \theta_-} \right|}{N}. \quad (13)$$

For this criterion, the absolute error between both sensitivity functions is calculated and summed over all times where the sensitivity is desired ( $N$ ).

- (iii) Maximum relative error (MRE).

$$\left| \frac{\frac{\partial y}{\partial \theta_+} - \frac{\partial y}{\partial \theta_-}}{\frac{\partial y}{\partial \theta_+}} \right|_{\text{MAX}}. \quad (14)$$

This criterion returns the maximum value of the relative difference between both sensitivity functions. One should be careful with this criterion because  $\partial y / \partial \theta_+$  or  $\partial y / \partial \theta_-$  may become 0. In these special cases the criterion returns 0.

- (iv) Sum of relative errors (SRE).

$$\frac{\sum \left| 1 - \frac{\frac{\partial y}{\partial \theta_-}}{\frac{\partial y}{\partial \theta_+}} \right|}{N}. \quad (15)$$

This criterion is also based on the ratio of the sensitivity functions. The ideal case is when this ratio equals 1, because then both sensitivity functions are equal. The criterion returns the sum of deviations from this ideal situation over all times where the sensitivity is desired ( $N$ ). Like the MRE criterion one should be careful if  $\partial y / \partial \theta_+$  becomes 0. In this special case no contribution is made to the total sum.

Figure 14 illustrates the use of these criteria for the sensitivity of the Benchmark autotrophic biomass ( $X_{B,A}$ ) to the maximum autotrophic growth rate ( $\mu_{mA}$ ) for perturbation factors ( $\xi$ ) ranging from 1E-01 to 1E-07. The optimal perturbation factor can be found when the criteria reach their minimum, in this case 1E-04. For larger perturbation factors ( $>1E-04$ ) the nonlinearity effect of the model influences the sensitivity calculations. This is illustrated in figure 15 for sensitivities calculated with a perturbation factor 1E-02 (1% parameter change). For comparison, the sensitivity function calculated with the optimal perturbation factor 1E-04 is also given. It is clear that  $\partial y / \partial \theta_-$  differs significantly from  $\partial y / \partial \theta_+$ . Figure 14 also illustrates the effect of

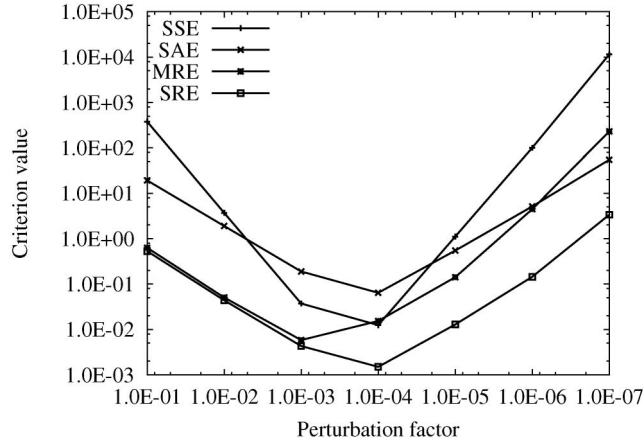


Figure 14. Criterion values for the sensitivity of the Benchmark autotrophic biomass ( $X_{B,A}$ ) to the maximum autotrophic growth rate ( $\mu_{mA}$ ) calculated with perturbation factors ranging from 1E-01 to 1E-07.

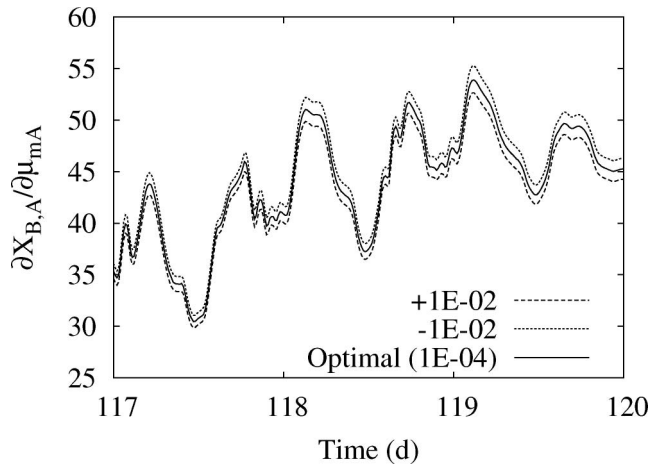


Figure 15. Nonlinear effect: sensitivity of the Benchmark autotrophic biomass ( $X_{B,A}$ ) to the maximum autotrophic growth rate ( $\mu_{mA}$ ) calculated with perturbation factors  $\pm 1E-02$  and  $1E-04$ .

numerical errors when perturbation factors lower than 1E-04 are selected. An example of this is given in figure 16 for a perturbation factor of 1E-06.

The problem of sensitivity evaluation would be quite easy if a fixed perturbation factor could be used. Let us therefore investigate whether the optimal perturbation factor is the same for other variables and parameters. For each model, table 2 gives the optimal perturbation factor ranges for all variables for a particular parameter. This table clearly shows that optimal perturbation factors are parameter dependent: some parameters have an optimal perturbation factor of 1E-01 others 1E-08. Applying a fixed perturbation factor to all parameters is not advisable. In the literature, however, this is frequently done [23–26].

We can also see that the optimal perturbation factor depends on the variable considered. For example, the optimal perturbation factors for the Benchmark  $\mu_{mH}$  are within the range of 1E-02 to 1E-04 for the SSE criterion. This means that the sensitivity of different variables to the same parameter ( $\mu_{mH}$ ) resulted in different optimal

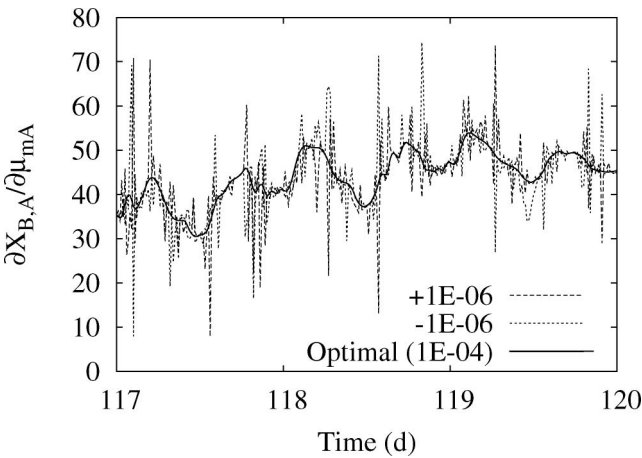


Figure 16. Numerical error effect: sensitivity of the Benchmark autotrophic biomass ( $X_{B,A}$ ) to the maximum autotrophic growth rate ( $\mu_{mA}$ ) calculated with perturbation factors  $\pm 1E-06$  and  $1E-04$ .

Table 2. Ranges of optimal perturbation factors for all variables to the given parameters.

|                  | SSE           | SAE           | MRE           | SRE           |
|------------------|---------------|---------------|---------------|---------------|
| <b>Monod</b>     |               |               |               |               |
| $\mu_{\max}$     | 1E-08         | 1E-08         | 1E-07 – 1E-08 | 1E-08         |
| $K_S$            | 1E-08         | 1E-07 – 1E-08 | 1E-07 – 1E-08 | 1E-08         |
| $Y$              | 1E-07         | 1E-07         | 1E-06 – 1E-07 | 1E-07         |
| $K_d$            | 1E-07         | 1E-07         | 1E-06 – 1E-07 | 1E-07         |
| <b>Anaerobic</b> |               |               |               |               |
| $k_1$            | 1E-01 – 1E-02 | 1E-02 – 1E-03 | 1E-01 – 1E-02 | 1E-02 – 1E-03 |
| $k_2$            | 1E-01 – 1E-02 | 1E-02 – 1E-03 | 1E-01 – 1E-02 | 1E-01 – 1E-02 |
| $k_3$            | 1E-02 – 1E-03 | 1E-03         | 1E-01 – 1E-02 | 1E-01 – 1E-03 |
| $\mu_{2\max}$    | 1E-03         | 1E-03         | 1E-02 – 1E-03 | 1E-03         |
| $K_{S_2}$        | 1E-02 – 1E-03 | 1E-03         | 1E-02 – 1E-03 | 1E-03         |
| $\alpha$         | 1E-03         | 1E-03         | 1E-03         | 1E-03         |
| <b>SBR</b>       |               |               |               |               |
| $Y_H$            | 1E-04         | 1E-04         | 1E-03 – 1E-04 | 1E-04         |
| $k_h$            | 1E-04         | 1E-04         | 1E-03 – 1E-04 | 1E-04         |
| $Y_{HNO_3}$      | 1E-04         | 1E-04         | 1E-03 – 1E-04 | 1E-03 – 1E-04 |
| $\mu_{NH}$       | 1E-04         | 1E-04         | 1E-02 – 1E-05 | 1E-04         |
| $Q_{PP}$         | 1E-02 – 1E-03 | 1E-02 – 1E-04 | 1E-02 – 1E-03 | 1E-02 – 1E-04 |
| $Y_{PO_4}$       | 1E-02 – 1E-03 | 1E-02 – 1E-03 | 1E-01 – 1E-02 | 1E-01 – 1E-03 |
| <b>Benchmark</b> |               |               |               |               |
| $\mu_{mH}$       | 1E-02 – 1E-04 | 1E-03 – 1E-04 | 1E-02 – 1E-04 | 1E-02 – 1E-04 |
| $\mu_{mA}$       | 1E-03 – 1E-04 | 1E-03 – 1E-04 | 1E-03 – 1E-04 | 1E-03 – 1E-04 |
| $Y_H$            | 1E-04         | 1E-04         | 1E-03 – 1E-04 | 1E-04         |
| $Y_A$            | 1E-03 – 1E-04 | 1E-03 – 1E-04 | 1E-02 – 1E-04 | 1E-03 – 1E-04 |
| $A$              | 1E-03 – 1E-04 | 1E-03 – 1E-04 | 1E-03 – 1E-04 | 1E-03 – 1E-04 |
| $H$              | 1E-02 – 1E-04 | 1E-03 – 1E-04 | 1E-02 – 1E-04 | 1E-02 – 1E-04 |
| $v_0$            | 1E-03         | 1E-03         | 1E-02 – 1E-04 | 1E-03         |
| $f_{ns}$         | 1E-02         | 1E-02 – 1E-03 | 1E-02         | 1E-02 – 1E-03 |

perturbation factors for that parameter. However, taking the average of the indicated range as the perturbation factor results in acceptable sensitivity functions for all variables.

From table 2, it can also be concluded that the different criteria indicate roughly the same optimal perturbation factors (also shown in figure 14). However, the ranges for

the MRE criterion are often different from the other criteria because this criterion is based on a maximum value while all other criteria are based on averaging.

### 4.3 Comparing different criteria

In order to investigate whether the value of a criterion obtained for a sensitivity calculation can be directly used to predict whether the sensitivity function calculation is valid, a closer look has to be taken at the criterion values obtained in the four case studies. Table 3 lists the minimum and maximum values of the different criteria for all calculated sensitivity functions and the minimum and maximum values of the different criteria at the optimal perturbation factors. In total, the criterion values of 634 sensitivity functions were calculated: for the Monod model, 8 sensitivity functions at 15 different perturbation factors (1E-01 to 1E-15); for the anaerobic digestion model, 18 sensitivity functions at 5 different perturbation factors (1E-01 to 1E-5); for the SBR model, 24 sensitivity functions at 6 different perturbation factors (1E-01 to 1E-6); for the Benchmark model, 40 sensitivity functions at 7 different perturbation factors (1E-01 to 1E-7).

From the table, it can be seen that the SSE and SAE criteria have a very broad range. This is caused by the use of the absolute values of the sensitivity functions. Sensitivity functions which are small in value result in small SSE and SAE values, while sensitivities which are large result in large SSE and SAE values. For the MRE and SRE criteria much narrower ranges are observed. This is because these criteria are based on relative differences between the sensitivity functions.

We can also see that the values of the criteria at the optimal perturbation factors show significant fluctuations. We might be tempted to use the upper bound of these ranges as the threshold value to decide if a sensitivity calculation is correct or not but the next section will show that this is not the optimal choice.

### 4.4 Selection of a useful threshold value

As a next step, expert knowledge was used to classify all 634 sensitivity functions in two categories: ‘good’ and ‘bad’. This was done based on visual inspection of both  $\partial y/\partial\theta_-$  and  $\partial y/\partial\theta_+$  (equation (11)). When  $\partial y/\partial\theta_-$  and  $\partial y/\partial\theta_+$  looked identical, the sensitivity function was classified as ‘good’ and when clear differences were noticed between  $\partial y/\partial\theta_-$  and  $\partial y/\partial\theta_+$  it was classified as ‘bad’. From this classification it became clear that not only sensitivity functions calculated with an optimal perturbation factor were ‘good’, but also some sensitivity functions which were calculated with a perturbation factor close to the optimal one.

Table 3. Ranges of criterion values for all calculated sensitivity functions and ranges of criterion values at the optimal perturbation factors.

| Criterion | Values for all sensitivity functions | Values at optimal perturbation factors |
|-----------|--------------------------------------|--|
| SSE       | 1.93E-16–1.72E+11                    | 1.93E-16–7.96E+02                      |
| SAE       | 8.19E-09–2.21E+05                    | 8.19E-09–2.02E+01                      |
| MRE       | 3.41E-07–7.20E+03                    | 3.41E-07–1.94E+01                      |
| SRE       | 1.57E-07–5.23E+01                    | 1.57E-07–3.99E-01                      |

Next, it was investigated whether a certain criterion value could be used as a threshold for automatic detection of ‘good’ and ‘bad’ sensitivity functions. Sensitivity functions with a criterion value lower than the threshold value are regarded as ‘good’, sensitivity functions with a criterion value higher than the threshold value are regarded as ‘bad’. Figures 17 to 20 show the percentages of ‘good’ and ‘bad’ sensitivity functions that were detected when imposing a certain threshold value for the different criteria. These percentages thus show which fraction of the ‘good’ and ‘bad’ sensitivity functions judged by expert knowledge was also detected by using the threshold value.

By means of example one can consider a threshold value of 1.0E-01 for the SRE criterion (figure 20). From the figure it can be seen that with this threshold value 95% of the ‘good’ sensitivity functions can be detected and only 65% of the ‘bad’ sensitivity functions. Similar conclusions can be drawn if the upper bound of the criterion values found at the optimal perturbation factors are considered (table 3).

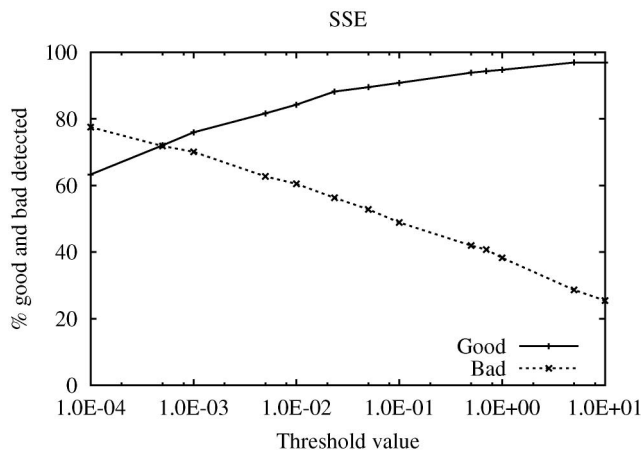


Figure 17. Percentages of ‘good’ and ‘bad’ sensitivity functions that were detected as a function of the threshold value for the SSE criterion.

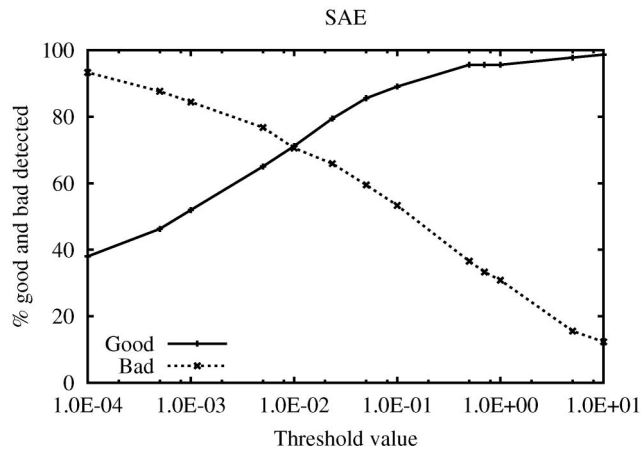


Figure 18. Percentages of ‘good’ and ‘bad’ sensitivity functions that were detected as a function of the threshold value for the SAE criterion.



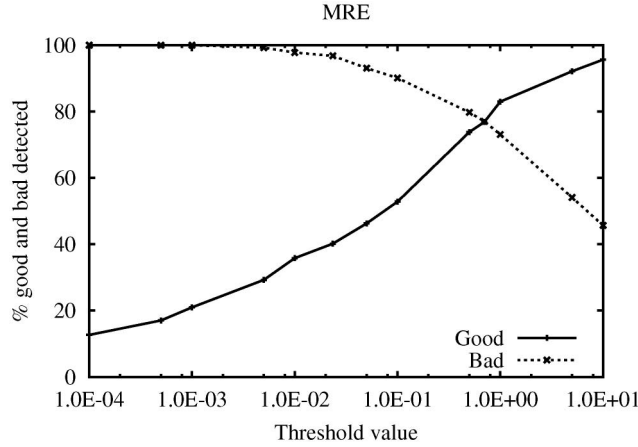


Figure 19. Percentages of 'good' and 'bad' expert knowledge sensitivity functions that were detected as a function of the threshold value for the MRE criterion.

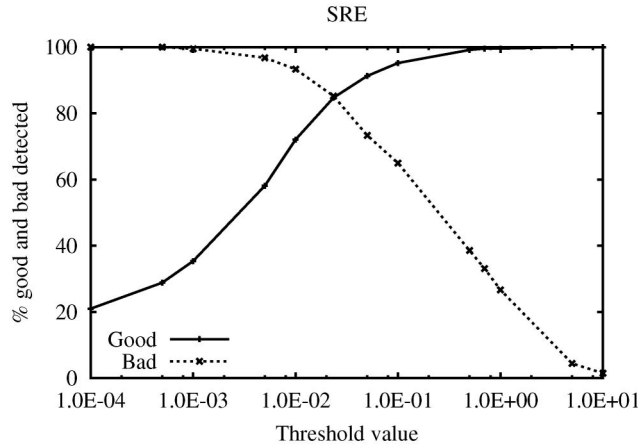


Figure 20. Percentages of 'good' and 'bad' expert knowledge sensitivity functions that were detected as a function of the threshold value for the SRE criterion.

The intersection of both curves on the graph corresponds with the threshold value at which a maximum amount of 'good' and 'bad' sensitivity functions are detected, e.g. for the SSE criterion a threshold value of  $2.35\text{E-}02$  with 85% detection was found. In other words, there is an 85% chance that a new sensitivity function with a SRE criterion value smaller than  $2.35\text{E-}02$  is 'good' and an 85% chance that a new sensitivity function with a SRE criterion value larger than  $2.35\text{E-}02$  is 'bad'. This threshold value could therefore be used to judge criterion values of future sensitivity functions.

From the figures it is also clear that the different criteria have different threshold values that correspond with the maximum detection level. The maximum detection levels are also different for each criterion: 72, 71, 77 and 85% for the SSE, SAE, MRE and SRE criterion respectively. The SRE criterion should preferably be used since its maximum detection level is the highest.

Figures 17 to 20 are based on the analysis of the combined sensitivity functions of all models (634 sensitivity functions). In order to know if the threshold value can be used

for other models, they need to be considered separately. In table 4 the threshold value and the corresponding maximum detection level for each model and each criterion are shown. The threshold values for the case in which all models are combined are also listed. Looking at the different criteria, it can be concluded that only the SRE criterion has an ‘optimal’ threshold value that is more or less constant for the different models. The maximum detection limit for this criterion is also larger and more constant compared to the other criteria. The only model that shows deviations is the Monod model, probably due to the limited number of sensitivity functions that were considered for this model. Based on these results, it can be concluded that the threshold value of 2.35E-02 for the SRE criterion can be used to judge with a high probability whether a sensitivity function calculation is ‘good’ or ‘bad’.

#### 4.5 Influence of integrator accuracy

All model evaluations used to calculate the sensitivity functions were performed using a Runge Kutta 4 Adaptive Stepsize Control integrator (RK4ASC) [27]. The adaptive stepsize option allows the integrator to decrease or increase the stepsize during the integration in order to maintain a user-defined accuracy between two successive integration steps. The influence of this integrator accuracy on the calculated sensitivity functions and optimal perturbation factors was investigated as well. Figure 21 shows the optimal perturbation factor for the sensitivity of the Benchmark nitrate concentration ( $S_{NO_3}$ ) to the heterotrophic yield coefficient ( $Y_H$ ) for different integrator settings. The left figure is the result of calculations with an integrator accuracy of 1E-09 and the right with an accuracy of 1E-06. An accuracy of 1E-09 has been used to produce all results shown before.

Table 4. Threshold values and corresponding maximum detection level for each model and each criterion.

|                     | Threshold value | % good and bad detected |
|---------------------|-----------------|-------------------------|
| <b>SSE</b>          |                 |                         |
| Monod               | 6.20E-06        | 85                      |
| Anaerobic digestion | 1.66E-03        | 57                      |
| SBR                 | 3.00E-03        | 80                      |
| Benchmark           | 7.10E-04        | 67                      |
| All models          | 5.00E-04        | 72                      |
| <b>SAE</b>          |                 |                         |
| Monod               | 1.10E-03        | 85                      |
| Anaerobic digestion | 4.33E-03        | 56                      |
| SBR                 | 2.10E-02        | 78                      |
| Benchmark           | 1.80E-02        | 66                      |
| All models          | 1.00E-02        | 71                      |
| <b>MRE</b>          |                 |                         |
| Monod               | 3.00E-02        | 83                      |
| Anaerobic digestion | 1.60E + 00      | 79                      |
| SBR                 | 1.20E + 00      | 80                      |
| Benchmark           | 9.60E-01        | 74                      |
| All models          | 7.00E-01        | 77                      |
| <b>SRE</b>          |                 |                         |
| Monod               | 3.00E-03        | 92                      |
| Anaerobic digestion | 2.40E-02        | 82                      |
| SBR                 | 4.70E-02        | 80                      |
| Benchmark           | 2.80E-02        | 84                      |
| All models          | 2.35E-02        | 85                      |

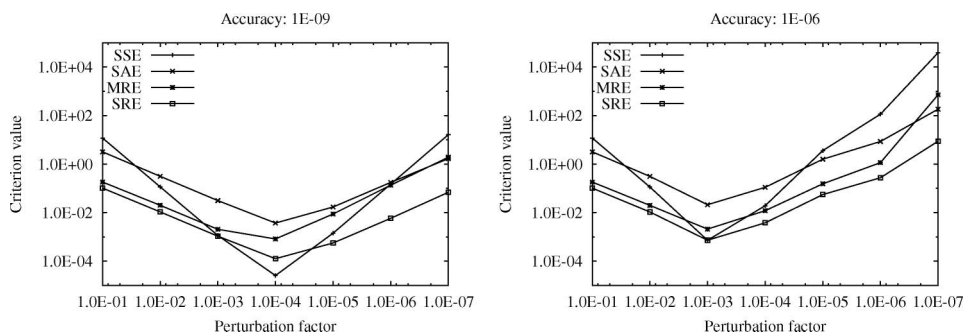


Figure 21. Optimal perturbation factor for the sensitivity of nitrate ( $S_{\text{NO}_3}$ ) to the heterotrophic yield ( $Y_{\text{H}}$ ) for different integrator accuracies: 1E-09 (left) and 1E-06 (right).

From both figures, it can be concluded that the accuracy has an influence on the optimal perturbation factor, 1E-04 for an accuracy of 1E-09 and 1E-03 for an accuracy of 1E-06. The accuracy also has an influence on the criterion values. All criterion values are lower for the 1E-09 accuracy and thus result in better sensitivity functions. For other models, parameters and variables this influence has also been demonstrated. It should be noted that higher integrator accuracies result in longer calculation times.

## 5. Conclusions

In this paper the finite difference sensitivity analysis technique was discussed in detail. Practically this technique was implemented using the central difference method. This method produces sensitivity functions around the nominal parameter values  $\theta$  and at the same time it allows one to assess the quality of the sensitivity function calculations. Different criteria were used as a measure for this quality.

The perturbation factor used in the finite difference method was found to be parameter dependent and to a lesser extent variable dependent. Among the proposed criteria the SRE criterion was found useful to assess the quality of sensitivity function calculations. A threshold value of 2.35E-02 for this criterion can be used to distinguish with high probability between 'good' and 'bad' sensitivity functions. It was also found that the integrator accuracy has a large influence on the calculated sensitivity functions and the optimal perturbation factors.

## Acknowledgements

This research was undertaken with the support of the Special Research Fund of the Ghent University and the IST Programme of the European Union (TELEMAC, project no. IST-2000-28156).

## References

- [1] Turanyi, T., 1990, Sensitivity analysis of complex kinetic systems, tools and applications. *Journal of Mathematical Chemistry*, **5**, 203–248.
- [2] Rabitz, H., Kramer, M. and Dacol, D., 1983, Sensitivity analysis in chemical kinetics. *Annual Review of Physical Chemistry*, **34**, 419–461.

- [3] Atherton, R.W., Schainker, R.B. and Ducot, E.R., 1975, Statistical sensitivity analysis of models for chemical-kinetics. *AIChE Journal*, **21**, 441–448.
- [4] Valko, P. and Vajda, S., 1984, An extended ODE solver for sensitivity calculations. *Computers and Chemistry*, **8**, 255–271.
- [5] Dickinson, R.P. and Gelinas, R.J., 1976, Sensitivity analysis of ordinary differential equation systems – a direct method. *Journal of Computational Physics*, **21**, 123–143.
- [6] Dougherty, E.P., Hwang, J.T. and Rabitz, H., 1979, Further developments and applications of the Green's function method of sensitivity analysis in chemical kinetics. *Journal of Chemical Physics*, **71**, 1794–1808.
- [7] Dougherty, E.P. and Rabitz, H., 1980, Computational kinetics and sensitivity analysis of hydrogen – oxygen combustion. *Journal of Chemical Physics*, **72**, 6571–6586.
- [8] Kramer, M.A., Calo, J.M. and Rabitz, H., 1981, An improved computational method for sensitivity analysis: Green's function method with 'AIM'. *Applied Mathematical Modelling*, **5**, 432–441.
- [9] Kramer, M.A., Rabitz, H., Calo, J.M. and Kee, R.J., 1984, Sensitivity analysis in chemical kinetics: recent developments and computational comparisons. *International Journal of Chemical Kinetics*, **16**, 559–578.
- [10] Dunker, A.M., 1981, Efficient calculation of sensitivity coefficients for complex atmospheric models. *Atmospheric Environment*, **15**, 1155–1161.
- [11] Dunker, A.M., 1984, The decoupled direct method for calculating sensitivity coefficients in chemical kinetics. *Journal of Chemical Physics*, **81**, 2385–2393.
- [12] Hwang, J.T., Dougherty, E.P., Rabitz, S. and Rabitz, H., 1978, The Green's function method of sensitivity analysis in chemical kinetics. *Journal of Chemical Physics*, **69**, 5180–5191.
- [13] Hwang, J.T., 1983, Sensitivity analysis in chemical kinetics by the method of polynomial approximations. *International Journal of Chemical Kinetics*, **15**, 959–987.
- [14] Hwang, J.T., 1985, A computational algorithm for the polynomial approximation method of sensitivity analysis in chemical kinetics. *Journal of the Chinese Chemical Society*, **32**, 253–261.
- [15] Hwang, D., Byun, D.W. and Odman, M.T., 1997, An automatic differentiation technique for sensitivity analysis of numerical advection schemes in air quality models. *Atmospheric Environment*, **31**, 879–888.
- [16] Vanhooren, H., Meirlaen, J., Amerlinck, Y., Claeys, F., Vangheluwe, H. and Vanrolleghem, P.A., 2003, WEST: modelling biological wastewater treatment. *Journal of Hydroinformatics*, **5**, 27–50.
- [17] Bernard, O., Hadj-Sadok, Z., Dochain, D., Genovesi, A. and Steyer, J.P., 2001, Dynamical model development and parameter identification for an anaerobic wastewater treatment process. *Biotechnology and Bioengineering*, **75**, 424–438.
- [18] Insel, G., Sin, G., Lee, D.S. and Vanrolleghem, P.A., 2004, A calibration methodology and model-based systems analysis for SBR's removing nutrients under limited aeration conditions. Presented at 3rd IWA International Conference on SBR, Queensland, Australia, 22–24 February 2004.
- [19] Henze, M., Grady, C.P.L., Gujer, W., Marais, G.V.R. and Matsuo, T., 1986, Activated sludge model No.1, IAWQ Scientific and Technical Report No. 1 (London: IAWQ).
- [20] Henze, M., Gujer, W., Mino, T., Matsuo, T., Wentzel, M.C., Marais, G.V.R. and Van Loosdrecht, M.C.M., 1999, Activated Sludge Model No.2d, ASM2d. *Water Science and Technology*, **39**, 165–182.
- [21] Copp, J.B., 2001, *The COST Simulation Benchmark: Description and Simulator Manual* (Luxembourg: Office for Official Publications of the European Community).
- [22] Takacs, I., Patry, G.G. and Nolasco, D., 1991, A dynamic model of the clarification thickening process. *Water Research*, **25**, 1263–1271.
- [23] Hoffmann, F., Posten, C. and Rinas, U., 2001, Kinetic model of *in vivo* folding and inclusion body formation in recombinant Escherichia coli. *Biotechnology and Bioengineering*, **72**, 315–322.
- [24] Marsili-Libelli, S., Ratini, P., Spagni, A. and Bortone, G., 2001, Implementation, study and calibration of a modified ASM2d for the simulation of SBR processes. *Water Science and Technology*, **43**, 69–76.
- [25] Reichert, P., 1994, Aquasim – a tool for simulation and data analysis of aquatic systems. *Water Science and Technology*, **30**, 21–30.
- [26] Saltelli, A., Chan, K. and Scott, E.M., 2000, *Sensitivity Analysis* (New York: Wiley).
- [27] Press, W.H., Teukolsky, S.A., Vetterling, W.T. and Flannery, B.P., 1992, *Numerical Recipes in C* (Cambridge: Cambridge University Press).